Meccanica
DOI 10.1007/s11012-011-9510-5

Numerical solutions of free convection boundary layer flow on a solid sphere with Newtonian heating in a micropolar fluid

M.Z. Salleh · R. Nazar · I. Pop

Received: 4 December 2010 / Accepted: 24 October 2011

Abstract In this paper, the problem of free convection boundary layer flow on a solid sphere in a micropolar fluid with Newtonian heating, in which the heat transfer from the surface is proportional to the local surface temperature, is considered. The transformed boundary layer equations in the form of partial differential equations are solved numerically using an implicit finite-difference scheme. Numerical solutions are obtained for the local wall temperature, the local skin friction coefficient, as well as the velocity, angular velocity and temperature profiles. The features of the flow and heat transfer characteristics for different values of the material or micropolar parameter K, the Prandtl number Pr and the conjugate parameter γ are analyzed and discussed.

M.Z. Salleh (✉)
Faculty of Industrial Science and Technology, Universiti Malaysia Pahang, 26300 UMP Kuantan, Pahang, Malaysia
e-mail: zukikuj@yahoo.com

R. Nazar
School of Mathematical Sciences, Faculty of Science and Technology, Universiti Kebangsaan Malaysia, 43600 UKM Bangi, Selangor, Malaysia

R. Nazar
Solar Energy Research Institute, Universiti Kebangsaan Malaysia, 43600 UKM Bangi, Selangor, Malaysia

I. Pop
Faculty of Mathematics, University of Cluj, 3400 Cluj, CP 253, Romania

Keywords Boundary layer · Free convection · Micropolar fluid · Newtonian heating · Sphere

Nomenclature

a	radius of the sphere
h_s	heat transfer parameter for Newtonian heating
C_f	skin friction coefficient
f	dimensionless stream function
g	acceleration due to gravity
Gr	Grashof number
H	angular velocity of micropolar fluid
j	microinertia density
K	material parameter of micropolar fluid
k	thermal conductivity
Pr	Prandtl number
Re	Reynolds number
T	fluid temperature
T_∞	ambient temperature
U_∞	free stream velocity
u, v	velocity components along the x and y directions, respectively
x, y	Cartesian coordinates along the sphere and normal to it, respectively

Greek Letters

β	thermal expansion coefficient
γ	conjugate parameter for Newtonian heating
μ	dynamic viscosity
ν	kinematic viscosity
θ	dimensionless temperature
κ	vortex viscosity

Published online: 16 November 2011

φ spin gradient viscosity
ρ fluid density
ψ stream function

1 Introduction

The essence of the theory of micropolar fluid flow lies in the extension of the constitutive equation for Newtonian fluid, so that more complex fluids such as particle suspensions, liquid crystal, animal blood, lubrication and turbulent shear flows can be described by this theory. The theory of micropolar fluid was first proposed by Eringen [1]. Extensive review of the theory and applications can be found in the review article by Ariman et al. [2]. Nazar et al. [3, 4] studied the free convection boundary layer flow on a solid sphere in a viscous and micropolar fluid with constant wall temperature (CWT) and constant heat flux (CHF), respectively. Generally, in modelling the convective boundary layer flow problems, the boundary conditions that were usually applied are constant wall temperature or heat flux. However, the Newtonian heating (NH) conditions have been used only recently by Merkin [5] to study the free convection boundary layer over vertical surfaces with Newtonian heating. The asymptotic solution near the leading edge and the full numerical solution along the whole plate domain have been obtained numerically, whilst the asymptotic solution far downstream along the plate has been obtained analytically. On the other hand, the situation with Newtonian heating occurs in many important engineering devices, for example in heat exchanger where the conduction in solid tube wall is greatly influenced by the convection in the fluid flowing over it. Further, for conjugate heat transfer around fins where the conduction within the fin and the convection in the fluid surrounding it must be simultaneously analyzed in order to obtain the vital design information and also in convection flows set up when the bounding surfaces absorb heat by solar radiation (see Chaudhary and Jain [6]).

Recent demands in heat transfer engineering have requested researchers to develop various new types of heat transfer equipments with superior performance, especially compact and light-weight ones. Increasing the need for small-size units, focuses have been cast on the effects of the interaction between developments of the thermal boundary layers in both fluid streams, and of axial wall conduction, which usually affects the heat exchanger performance. Since the early paper by Luikov et al. [7], many contributions to the topic of conjugate heat transfer have been produced. Excellent reviews of the topics of conjugate heat transfer problems can be found in the book by Martynenko and Khramtsov [8] and the review paper by Kimura et al. [9]. Recently, Salleh et al. [10–14] and Merkin et al. [15] considered the forced convection boundary layer flow at a forward stagnation point, free, mixed and forced convection boundary layer flows on a sphere, horizontal circular cylinder and stretching sheet with Newtonian heating, respectively. These problems have been extended to viscous and micropolar fluids by many investigators such as [16–20] in various ways either with constant wall temperature and concentration, constant heat and mass fluxes or with heat generation.

Therefore, the aim of the present paper is to study the free convection boundary layer flow on a solid sphere with Newtonian heating in a micropolar fluid. The full governing boundary layer equations are first transformed into a system of non-dimensional equations via the non-dimensional variables, and then into non-similar partial differential equations before they are solved numerically by the Keller-box method, an implicit finite-difference scheme as described in the book by and Cebeci and Bradshaw [21]. Results are presented for the local wall temperature, the local skin friction coefficient, as well as the velocity, angular velocity and temperature profiles.

2 Mathematical model

Consider a heated sphere of radius a, which is immersed in a viscous and incompressible micropolar fluid of ambient temperature T_∞. The surface of the sphere is subjected to a Newtonian heating (NH). We assume that the equations are subjected to a Newtonian heating of the form proposed by Merkin [5]. Under the Boussinesq and boundary layer approximations, the basic equations are (see Eringen [1], Nazar et al. [3, 4])

$$\frac{\partial}{\partial \bar{x}}(\bar{r}\bar{u}) + \frac{\partial}{\partial \bar{y}}(\bar{r}\bar{v}) = 0, \tag{1}$$

$$\rho\left(\bar{u}\frac{\partial \bar{u}}{\partial \bar{x}} + \bar{v}\frac{\partial \bar{u}}{\partial \bar{y}}\right) = (\mu+\kappa)\frac{\partial^2 \bar{u}}{\partial \bar{y}^2} + \rho g\beta(T-T_\infty)\sin\left(\frac{\bar{x}}{a}\right) + \kappa\frac{\partial \bar{H}}{\partial \bar{y}}, \tag{2}$$

$$\rho j\left(\bar{u}\frac{\partial \bar{H}}{\partial \bar{x}}+\bar{v}\frac{\partial \bar{H}}{\partial \bar{y}}\right)=-\kappa\left(2\bar{H}+\frac{\partial \bar{u}}{\partial \bar{y}}\right)+\varphi\frac{\partial^2 \bar{H}}{\partial \bar{y}^2}, \quad (3)$$

$$\bar{u}\frac{\partial T}{\partial \bar{x}}+\bar{v}\frac{\partial T}{\partial \bar{y}}=\frac{\nu}{Pr}\frac{\partial^2 T}{\partial \bar{y}^2}, \quad (4)$$

where $\bar{r}(\bar{x})=a\sin(\bar{x}/a)$ and we assume that $\varphi=(\mu+(\kappa/2))j$. The boundary conditions of (1)–(4) are

$$\begin{aligned}&\bar{u}=\bar{v}=0, \qquad \frac{\partial T}{\partial \bar{y}}=-h_s T,\\ &\bar{H}=-n\frac{\partial \bar{u}}{\partial \bar{y}} \quad \text{at } \bar{y}=0,\\ &\bar{u}\to 0, \qquad T\to T_\infty, \qquad \bar{H}\to 0 \quad \text{as } \bar{y}\to\infty,\end{aligned} \quad (5)$$

where $\bar{u}$ and $\bar{v}$ are the velocity components along the $\bar{x}$ and $\bar{y}$ directions, respectively, T is the local temperature, ρ is the fluid density, g is the gravity acceleration, β is the thermal expansion coefficient, $\nu=\frac{\mu}{\rho}$ is the kinematic viscosity, μ is the dynamic viscosity, κ is the vortex viscosity, $\bar{H}$ is the angular velocity of micropolar fluid, j is the microinertia density, φ is the spin gradient viscosity, Pr is the Prandtl number and h_s is a heat transfer parameter for Newtonian heating.

It is worth mentioning that in boundary conditions (5), n is a constant and $0\le n\le 1$. The value $n=0$, which indicates $\bar{H}=0$ at the wall, represents concentrated particle flows in which the particle density is sufficiently great that microelements close to the wall are unable to rotate or it is called "strong" concentration of microelements [22, 23]. The case corresponding to $n=\frac{1}{2}$ results in the vanishing of antisymmetric part of the stress tensor and represents "weak" concentration of microelements [24]. In this case, the particle rotation is equal to fluid vorticity at the boundary for fine particle suspension. When $n=1$, we have flows which are representative of turbulent boundary layer [25]. The case of $n=\frac{1}{2}$ is considered in the present study, in order to compare some results with those of Nazar et al. [3, 4] for the CWT and CHF cases in viscous fluids, respectively, who also considered the case of $n=\frac{1}{2}$ (refer [11]). It is worth mentioning that the correct boundary condition to be applied to the spin is still an open question. However, the most common boundary conditions used in the literature are the vanishing of the spin on the boundary, the so-called strong interaction ($n=0$) and the opposite extreme, the weak interaction ($n=\frac{1}{2}$), which is the vanishing of the momentum stress on the boundary [23].

We introduce now the following non-dimensional variables (Nazar et al. [3]):

$$\begin{aligned}&x=\frac{\bar{x}}{a}, \qquad y=Gr^{1/4}\left(\frac{\bar{y}}{a}\right), \qquad r=\frac{\bar{r}}{a},\\ &u=\left(\frac{a}{\nu}\right)Gr^{-1/2}\bar{u}, \qquad v=\left(\frac{a}{\nu}\right)Gr^{-1/4}\bar{v},\\ &H=\left(\frac{a^2}{\nu}\right)Gr^{-3/4}\bar{H}, \qquad \theta=\frac{T-T_\infty}{T_\infty},\end{aligned} \quad (6)$$

where $Gr=\frac{g\beta T_\infty a^3}{\nu^2}$ is the Grashof number for Newtonian heating (NH). The microinertia density j is taken to be $j=a^2Gr^{-1/2}$. Substituting variables (6) into (1)–(4) then become

$$\frac{\partial}{\partial x}(ru)+\frac{\partial}{\partial y}(rv)=0 \quad (7)$$

$$u\frac{\partial u}{\partial x}+v\frac{\partial u}{\partial y}=(1+K)\frac{\partial^2 u}{\partial y^2}+\theta\sin x+K\frac{\partial H}{\partial y} \quad (8)$$

$$u\frac{\partial H}{\partial x}+v\frac{\partial H}{\partial y}=-K\left(2H+\frac{\partial u}{\partial y}\right)+\left(1+\frac{K}{2}\right)\frac{\partial^2 H}{\partial y^2} \quad (9)$$

$$u\frac{\partial \theta}{\partial x}+v\frac{\partial \theta}{\partial y}=\frac{1}{Pr}\frac{\partial^2 \theta}{\partial y^2} \quad (10)$$

where K is the material or micropolar parameter defined as $K=\frac{\kappa}{\mu}$. The boundary conditions are

$$\begin{aligned}&u=v=0, \qquad \frac{\partial \theta}{\partial y}=-\gamma(1+\theta),\\ &H=-\frac{1}{2}\frac{\partial u}{\partial y} \quad \text{at } y=0\\ &u\to 0, \qquad \theta\to 0, \qquad H\to 0 \quad \text{as } y\to\infty\end{aligned} \quad (11)$$

where $\gamma=ah_sGr^{-1/4}$ represents the conjugate parameter for Newtonian heating. We notice that (11) gives $\theta=0$ when $\gamma=0$, corresponding to having $h_s=0$ and hence no heating from the sphere exists (see Salleh et al. [11, 12]). To solve (7) to (10), subjected to the boundary conditions (11), we assume the following variables:

$$\begin{aligned}&\psi=xr(x)f(x,y), \qquad \theta=\theta(x,y),\\ &H=xh(x,y)\end{aligned} \quad (12)$$

where ψ is the stream function defined as

$$u=\frac{1}{r}\frac{\partial \psi}{\partial y} \quad \text{and} \quad v=-\frac{1}{r}\frac{\partial \psi}{\partial x} \quad (13)$$

which satisfies the continuity equation (7). Thus, (8) to (10) then become

$$(1+K)\frac{\partial^3 f}{\partial y^3}+\left(1+\frac{x}{\sin x}\cos x\right)f\frac{\partial^2 f}{\partial y^2}-\left(\frac{\partial f}{\partial y}\right)^2+\frac{\sin x}{x}\theta+K\frac{\partial h}{\partial y}=x\left(\frac{\partial f}{\partial y}\frac{\partial^2 f}{\partial x\partial y}-\frac{\partial f}{\partial x}\frac{\partial^2 f}{\partial y^2}\right), \quad (14)$$

$$\left(1+\frac{K}{2}\right)\frac{\partial^2 h}{\partial y^2}+\left(1+\frac{x}{\sin x}\cos x\right)f\frac{\partial h}{\partial y}-\frac{\partial f}{\partial y}h-K\left(2h+\frac{\partial^2 f}{\partial y^2}\right)=x\left(\frac{\partial f}{\partial y}\frac{\partial h}{\partial x}-\frac{\partial f}{\partial x}\frac{\partial h}{\partial y}\right), \quad (15)$$

$$\frac{1}{Pr}\frac{\partial^2\theta}{\partial y^2}+\left(1+\frac{x}{\sin x}\cos x\right)f\frac{\partial\theta}{\partial y}=x\left(\frac{\partial f}{\partial y}\frac{\partial\theta}{\partial x}-\frac{\partial f}{\partial x}\frac{\partial\theta}{\partial y}\right), \quad (16)$$

subject to the boundary conditions

$$f=\frac{\partial f}{\partial y}=0, \qquad \frac{\partial\theta}{\partial y}=-\gamma(1+\theta),$$
$$h=-\frac{1}{2}\frac{\partial^2 f}{\partial y^2} \quad \text{at } y=0 \quad (17)$$
$$\frac{\partial f}{\partial y}\to 0, \qquad \theta\to 0, \qquad h\to 0 \quad \text{as } y\to\infty$$

At the lower stagnation point of the sphere, $x\approx 0$, (14) to (16) reduce to the following ordinary differential equations:

$$(1+K)f'''+2ff''-f'^2+\theta+Kh'=0 \quad (18)$$
$$\left(1+\frac{K}{2}\right)h''+2fh'-f'h-K(2h+f'')=0 \quad (19)$$
$$\frac{1}{Pr}\theta''+2f\theta'=0 \quad (20)$$

and the boundary conditions become

$$f(0)=f'(0)=0, \qquad \theta'(0)=-\gamma\big(1+\theta(0)\big),$$
$$h(0)=-\frac{1}{2}f''(0) \quad \text{at } y=0, \quad (21)$$
$$f'\to 0, \qquad \theta\to 0, \qquad h\to 0 \quad \text{as } y\to\infty$$

where primes denote differentiation with respect to y. The physical quantities of interest in this problem are the local skin friction coefficient, C_f and the local wall temperature, $\theta_w(x)$, which are given by (when $\gamma=1$)

$$C_f=\left(1+\frac{K}{2}\right)x\frac{\partial^2 f}{\partial y^2}(x,0),$$
$$\theta_w(x)=-1-\frac{\partial\theta}{\partial y}(x,0) \quad (22)$$

where $C_f=\tau_w/(\rho U_\infty{}^2)$ is the skin friction coefficient and $\tau_w=[(\mu+\kappa)(\partial\bar{u}/\partial\bar{y})+\kappa\bar{H}]_{\bar{y}=0}$ is the wall shear stress.

At the lower stagnation point of the sphere, $x\approx 0$, the skin friction coefficient and the wall temperature are measured by $f''(0)$ and $\theta(0)$, respectively.

3 Solution procedure

Equations (14) to (16) subject to boundary conditions (17) are solved numerically using the Keller-box method as described in the book by Cebeci and Bradshaw [21]. The solution is obtained by the following four steps:

- reduce (14) to (16) to a first-order system,
- write the difference equations using central differences,
- linearize the resulting algebraic equations by Newton's method, and write them in the matrix-vector form,
- solve the linear system by the block tridiagonal elimination technique.

The step size Δy in y, and the edge of the boundary layer y_∞ had to be adjusted for different values of parameters to maintain accuracy.

4 Results and discussion

Equations (14) to (16) subject to the boundary conditions (17) are solved numerically using the Keller-box method for the case of Newtonian heating (NH) with four parameters considered, namely the material parameter K, the Prandtl number Pr, the conjugate parameter γ and the coordinate running along the surface of the sphere, x. The numerical solution starts at the lower stagnation point of the sphere, $x\approx 0$, and proceeds round the sphere up to the point $x=120°$. Values of K considered are $K=0$ (Newtonian fluid), 1, 2 and 3 (micropolar fluid) and values of Pr considered are $Pr=0.7$, 1 and 7 at different positions $x=0°$, 10°, 20°, 30°, 40°, 50°, 60°, 70°, 80°, 90°, 100°, 110°, and 120°. It is worth mentioning that small values of Pr ($\ll 1$) physically correspond to liquid metals, which have high thermal conductivity but low viscosity, while large values of Pr ($\gg 1$) correspond to high-viscosity oils. It is worth pointing out that specifically, Prandtl number $Pr=0.7$, 1.0 and 7.0 correspond to air, electrolyte solution such as salt water and water, respectively.

The values of the skin friction coefficient and the wall temperature in a Newtonian fluid ($K = 0$) and $\gamma = 1$ are shown in Table 1. In order to verify the accuracy of the present method, the present results are compared with those reported by Salleh et al. [12]. It is found that the agreement between the previously published results with the present ones is very good. We can conclude that this method works efficiently for the present problem and we are also confident that the results presented here are accurate.

Tables 2 and 3 present the values of the wall temperature, $\theta(0)$ and the skin friction coefficient, $f''(0)$ at the lower stagnation point of the sphere for various values of K when $Pr = 0.7$, 1 and 7 and $\gamma = 1$, respectively. It is found that for fixed Pr, as K increases, the value of $\theta(0)$ increases but $f''(0)$ decreases. Also, it is found that for fixed K, as Pr increases, both $\theta(0)$ and $f''(0)$ decrease. From these tables, the values of $\theta(0)$ are higher for micropolar fluid ($K \neq 0$) than those for a Newtonian fluid ($K = 0$) but the values of $f''(0)$ are lower for micropolar fluid ($K \neq 0$) than those for a Newtonian fluid ($K = 0$).

Tables 4 to 7 present the values of the local wall temperature $\theta_w(x)$ and the local skin friction coefficient C_f for various values of x when $Pr = 0.7$, 1 and 7, $K = 0$ and 1 and $\gamma = 1$, respectively. It is found that, for fixed K, as Pr increases, both the $\theta_w(x)$ and C_f decrease. From these tables, for a fixed Pr, as x increases, i.e. from the lower stagnation point of the sphere, $x \approx 0$, and proceeds round the sphere up to the point $x = 120°$, both the values of $\theta_w(x)$ and C_f increase. On the other hand, the values of $\theta_w(x)$ and C_f are higher for micropolar fluid ($K = 1$) than those for a Newtonian fluid ($K = 0$).

The graphs of $f''(x, 0)$ and $\theta(x, 0)$ for some values of Pr when $K = 1$ and $\gamma = 1$ are plotted in Figs. 1 and 2, respectively. It is found that, as Pr increases, both $f''(x, 0)$ and $\theta(x, 0)$ decrease. For small values of Pr ($\ll 1$) the difference value changing is higher than for large values of Pr ($\gg 1$) and it is seen that the surface temperature is very sensitive to the Prandtl

Table 1 Values of the skin friction coefficient $f''(0)$ and the wall temperature $\theta(0)$ at the lower stagnation point of the sphere, $x \approx 0$, when $Pr = 0.7$, 1 and 7, $K = 0$ (Newtonian fluid) and $\gamma = 1$

Pr	$f''(0)$		$\theta(0)$	
	Salleh et al. [12]	Present	Salleh et al. [12]	Present
0.7	8.9610	8.9609	26.4590	26.4584
1	6.1411	6.1409	17.2876	17.2861
7	1.2487	1.2489	3.3635	3.3651

Table 2 Values of the wall temperature $\theta(0)$ at the lower stagnation point of the sphere, $x \approx 0$, for various values of K when $Pr = 0.7$, 1 and 7 and $\gamma = 1$

Pr	0.7	1	7
K	Present	Present	Present
0	26.4584	17.2861	3.3651
1	38.3841	25.2867	4.6309
2	49.1395	32.4395	5.5150
3	59.3500	39.2872	6.4152

Table 3 Values of the skin friction coefficient $f''(0)$ at the lower stagnation point of the sphere, $x \approx 0$, for various values of K when $Pr = 0.7$, 1 and 7 and $\gamma = 1$

Pr	0.7	1	7
K	Present	Present	Present
0	8.9609	6.1409	1.2489
1	7.4816	5.1336	0.9790
2	6.8457	4.6987	0.8600
3	6.4721	4.4437	0.7900

Table 4 Values of the local wall temperature, $\theta_w(x)$ for various values of x when $Pr = 0.7$, 1 and 7, $K = 0$ and $\gamma = 1$

Pr	0.7	1	7
x	Present	Present	Present
0°	26.4590	17.2876	3.3635
10°	56.8602	36.1847	5.4172
20°	59.4033	37.7239	5.5141
30°	61.1367	38.7087	5.5857
40°	62.7065	39.6506	5.6687
50°	64.3987	40.7060	5.7880
60°	66.2689	41.8821	5.9499
70°	68.5102	43.2987	6.1331
80°	71.1541	44.9755	6.3583
90°	74.2967	46.9734	6.6289
100°	78.0623	49.3714	6.9555
110°	82.6233	52.2792	7.3530
120°	88.2340	55.8588	7.8427

Table 5 Values of the local skin friction coefficient, C_f for various values of x when $Pr = 0.7$, 1 and 7, $K = 0$ and $\gamma = 1$

Pr	0.7	1	7
x	Present	Present	Present
0°	0.0000	0.0000	0.0000
10°	2.8206	1.8939	0.2909
20°	5.7090	3.8817	0.5854
30°	8.7332	5.8418	0.8785
40°	11.5864	7.7431	1.1618
50°	14.3102	9.5616	1.4186
60°	16.7934	11.2211	1.6778
70°	19.1415	12.7925	1.9052
80°	21.2356	14.1966	2.1172
90°	23.0291	15.4035	2.3029
100°	24.4695	16.3780	2.4569
110°	25.4947	17.0803	2.5741
120°	26.0269	17.4585	2.6466

Table 6 Values of the local wall temperature, $\theta_w(x)$ for various values of x when $Pr = 0.7$, 1 and 7, $K = 1$ and $\gamma = 1$

Pr	0.7	1	7
x	Present	Present	Present
0°	38.3841	25.2867	4.6309
10°	87.8744	56.9775	8.1822
20°	92.0951	59.5915	8.3870
30°	94.7977	61.2801	8.5329
40°	97.2352	62.8666	8.6958
50°	100.0066	64.5873	8.8945
60°	102.9836	66.4993	9.1265
70°	106.5506	68.7977	9.4142
80°	110.7602	71.5168	9.7615
90°	115.7666	74.7564	10.1802
100°	121.7694	78.6456	10.6867
110°	129.0451	83.3636	11.3034
120°	135.5077	89.1734	12.0632

number variations. To get a physically acceptable solution, Pr must be greater than or equals to some critical value, say Pr_c, i.e. $Pr \geq Pr_c$, depending on γ. It can be seen from these figures that $f''(x, 0)$ and $\theta(x, 0)$ become large as Pr approaches the critical value $Pr_c = 0.025$ when $\gamma = 1$.

Figure 3 illustrates the variation of the wall temperature $\theta(x, 0)$ with conjugate parameter γ when $Pr = 7$ and $K = 1$. Also, to get a physically acceptable solu-

Table 7 Values of the local skin friction coefficient, C_f for various values of x when $Pr = 0.7$, 1 and 7, $K = 1$ and $\gamma = 1$

Pr	0.7	1	7
x	Present	Present	Present
0°	0.0000	0.0000	0.0000
10°	3.7233	2.5231	0.3796
20°	7.6625	5.1853	0.7686
30°	11.5608	7.8181	1.1500
40°	15.2420	10.3761	1.5207
50°	18.9680	12.8203	1.8764
60°	22.2741	15.0547	2.2030
70°	25.4072	17.1748	2.5154
80°	28.2108	19.0749	2.7984
90°	30.6248	20.7150	3.0470
100°	32.5814	22.0499	3.2546
110°	34.0003	23.0267	3.4144
120°	34.6476	23.5785	3.5171

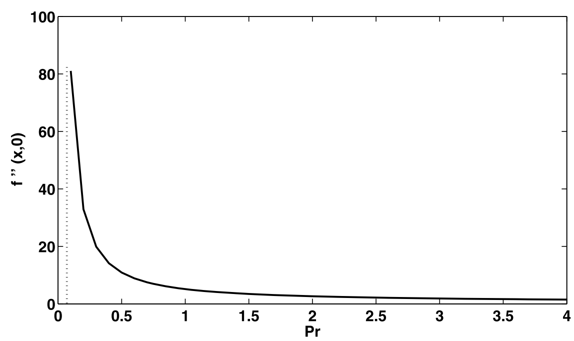

Fig. 1 Graph of $f''(x, 0)$ with Prandtl number Pr when $K = 1$ and $\gamma = 1$

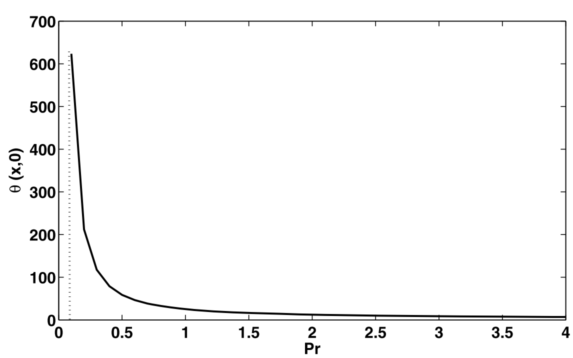

Fig. 2 Graph of $\theta(x, 0)$ with Prandtl number Pr when $K = 1$ and $\gamma = 1$

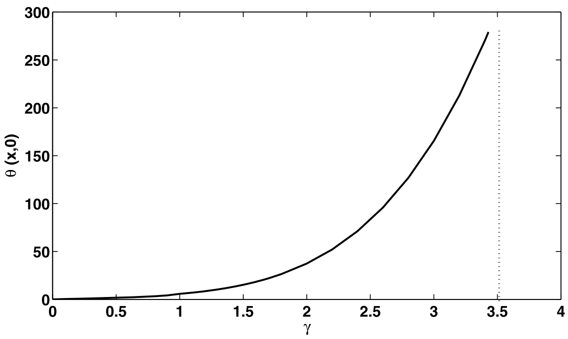

Fig. 3 Variation of the wall temperature $\theta(x, 0)$ with conjugate parameter γ when $Pr = 7$ and $K = 1$

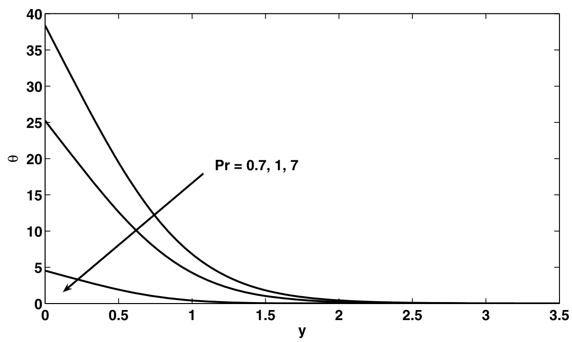

Fig. 4 Temperature profiles near the lower stagnation point of the sphere, $x \approx 0$, when $Pr = 0.7$, 1 and 7, $K = 1$ and $\gamma = 1$

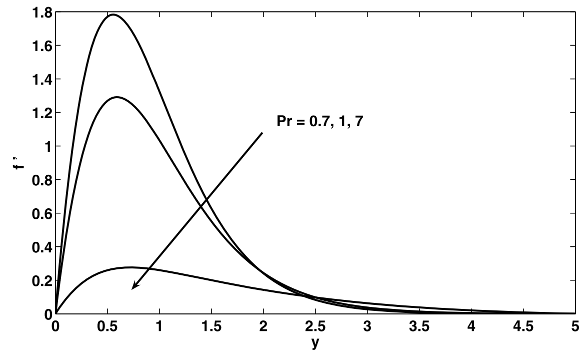

Fig. 5 Velocity profiles near the lower stagnation point of the sphere, $x \approx 0$, when $Pr = 0.7$, 1 and 7, $K = 1$ and $\gamma = 1$

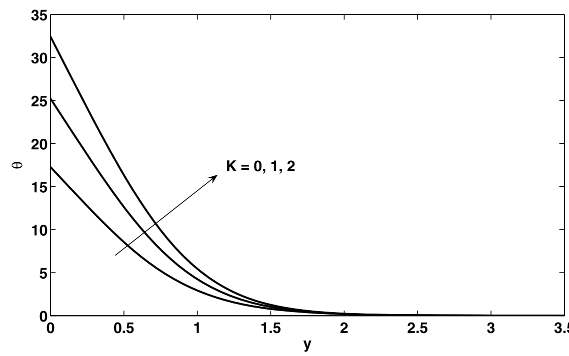

Fig. 6 Temperature profiles near the lower stagnation point of the sphere, $x \approx 0$, when $K = 0$, 1 and 2, $Pr = 1$ and $\gamma = 1$

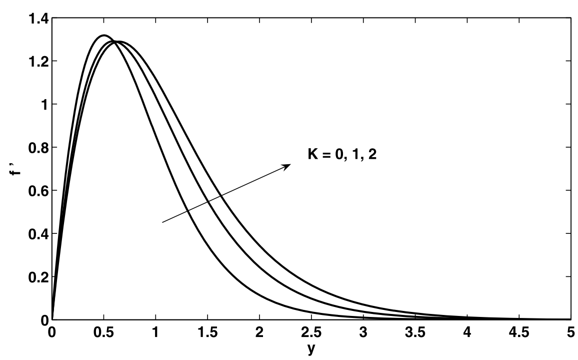

Fig. 7 Velocity profiles near the lower stagnation point of the sphere, $x \approx 0$, when $K = 0$, 1 and 2, $Pr = 1$ and $\gamma = 1$

tion, γ must be less than or equals to some critical value, say γ_c, i.e. $\gamma \leq \gamma_c$, depending on Pr. It can be seen from this figure that $\theta(x, 0)$ becomes large as γ approaches the critical value $\gamma_c = 3.5020$ when $Pr = 7$ and $K = 1$.

Figures 4 and 5 display the temperature and velocity profiles, respectively, near the lower stagnation point of the sphere when $Pr = 0.7$, 1 and 7, $K = 1$ and $\gamma = 1$. From Fig. 4, it is found that as Pr increases, the temperature profiles decrease and also the thermal boundary layer thickness decreases. This is because for small values of the Prandtl number Pr ($\ll$1), the fluid is highly conductive. Physically, if Pr increases, the thermal diffusivity decreases and this phenomenon leads to the decreasing manner of the energy transfer ability that reduces the thermal boundary layer. On the other hand, from Fig. 5 it is shown that for fixed K, as Pr increases, the velocity profiles decrease.

Temperature and velocity profiles near the lower stagnation point of the sphere for some values of K, namely $K = 0$, 1 and 2 when $Pr = 1$ and $\gamma = 1$ are plotted in Figs. 6 and 7, respectively. It is found that when Pr is fixed, as K increases, both the temperature and velocity profiles increase. Figures 8 and 9 display the angular velocity or microrotation profiles near the lower stagnation point of the sphere for some values of

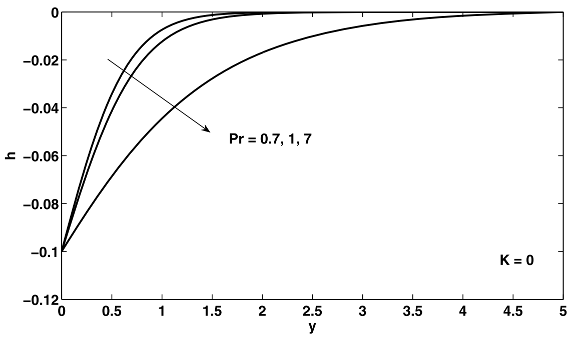

Fig. 8 Angular velocity profiles near the lower stagnation point of the sphere, $x \approx 0$, when $Pr = 0.7$, 1 and 7, $K = 0$ and $\gamma = 1$

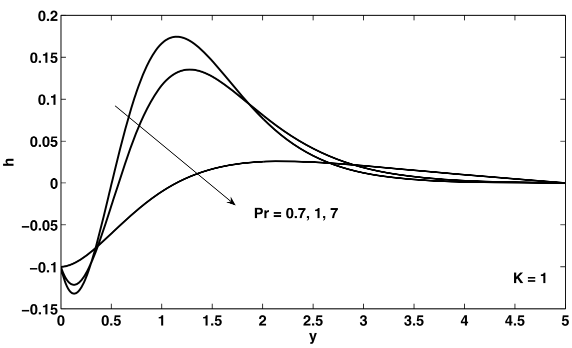

Fig. 9 Angular velocity profiles near the lower stagnation point of the sphere, $x \approx 0$, when $Pr = 0.7$, 1 and 7, $K = 1$ and $\gamma = 1$

Pr, namely $Pr = 0.7$, 1 and 7 when $K = 0$ and $K \neq 0$ and $\gamma = 1$, respectively. These figures show that the angular velocity is completely negative for $K = 0$, while it may be positive for $K = 1$ (or for other values of $K \neq 0$). It is also noticed from these figures that as the material parameter K increases, the angular velocity profiles decrease.

5 Conclusions

In this paper, we have numerically studied the problem of free convection boundary layer flow on a sphere in a micropolar fluid with Newtonian heating. We are interested to see how the material parameter K, the Prandtl number Pr and conjugate parameter γ affect the flow and heat transfer characteristics. We can conclude that:

- when Pr and γ are fixed, as K increases, the temperature and velocity profiles increase, while when K and γ are fixed, as Pr increases, the temperature, velocity and angular velocity profiles decrease;
- when Pr and γ are fixed, the values of θ_w and C_f are higher for micropolar fluids ($K \neq 0$) than those for a Newtonian fluid ($K = 0$);
- when K and γ are fixed, as Pr increases, both the values of θ_w and C_f decrease;
- to get a physically acceptable solution, Pr must be greater than Pr_c depending on γ, and also, γ must be less than γ_c depending on Pr.

Acknowledgement The authors gratefully acknowledge the financial supports received from the Ministry of Higher Education, Malaysia (UKM-ST-07-FRGSS0036-2009) and the Universiti Malaysia Pahang (RDU110108). They also wish to express their very sincere thanks to the reviewers for the valuable comments and suggestions.

References

1. Eringen AC (1966) Theory of micropolar fluids. J Math Mech 16:1–18
2. Ariman T, Turk MA, Sylvester ND (1974) Application of microcontinuum fluid mechanics. Int J Eng Sci 12:273–293
3. Nazar R, Amin N, Grosan T, Pop I (2002) Free convection boundary layer on an isothermal sphere in a micropolar fluid. Int Commun Heat Mass Transf 29:377–386
4. Nazar R, Amin N, Grosan T, Pop I (2002) Free convection boundary layer on a sphere with constant surface heat flux in a micropolar fluid. Int Commun Heat Mass Transf 29:1129–1138
5. Merkin JH (1994) Natural convection boundary-layer flow on a vertical surface with Newtonian heating. Int J Heat Fluid Flow 15:392–398
6. Chaudhary RC, Jain P (2007) An exact solution to the unsteady free convection boundary-layer flow past an impulsively started vertical surface with Newtonian heating. J Eng Phys Thermophys 80:954–960
7. Luikov AV, Aleksashenko VA, Aleksashenko AA (1971) Analytic methods of solution of conjugate problems in convection heat transfer. Int J Heat Mass Transf 14:1047–1056
8. Martynenko OG, Khramtsov PP (2005) Free-convective heat transfer. Springer, Berlin
9. Kimura S, Kiwata T, Okajima A, Pop I (1997) Conjugate natural convection in porous media. Adv Water Resour 20:111–126
10. Salleh MZ, Nazar R, Pop I (2009) Forced convection boundary layer flow at a forward stagnation point with Newtonian heating. Chem Eng Commun 196:987–996
11. Salleh MZ, Nazar R, Pop I (2010) Mixed convection boundary layer flow about a solid sphere with Newtonian heating. Arch Mech 62:283–303
12. Salleh MZ, Nazar R, Pop I (2010) Modeling of free convection boundary layer flow on a sphere with Newtonian heating. Acta Appl Math 112:263–274
13. Salleh MZ, Nazar R, Pop I (2010) Modelling of boundary layer flow and heat transfer over a stretching sheet with Newtonian heating. J Taiwan Inst Chem Eng 41(6):651–655

14. Salleh MZ, Nazar R, Arifin NM, Merkin JH, Pop I (2011) Forced convection heat transfer over a horizontal circular cylinder with Newtonian heating. J Eng Math 69(1):101–110
15. Merkin JH, Nazar R, Pop I (2011) The development of forced convection heat transfer near a forward stagnation point with Newtonian heating. J Eng Math. doi:10.1007/s10665-011-9487-z
16. Cheng CY (2008) Natural convection heat and mass transfer from a sphere in micropolar fluids with constant wall temperature and concentration. Int Commun Heat Mass Transf 35:750–755
17. Cheng CY (2010) Nonsimilar solutions for double-diffusion boundary layers on a sphere in micropolar fluids with constant wall heat and mass fluxes. Appl Math Model 34:1892–1900
18. Miraj M, Alim MA, Andallah LS (2011) Effects of pressure work and radiation on natural convection flow around a sphere with heat generation. Int Commun Heat Mass Transf 38:911–916
19. Prasad VR, Vasu B, Anwar Beg O, Parshad RD (2012) Thermal radiation effects on magnetohydrodynamic free convection heat and mass transfer from a sphere in a variable porosity regime. Commun Nonlinear Sci Numer Simul 17:654–671
20. Turkyilmazoglu M (2011) Numerical and analytical solutions for the flow and heat transfer near the equator of an MHD boundary layer over a porous rotating sphere. Int J Therm Sci 50:831–842
21. Cebeci T, Bradshaw P (1988) Physical and computational aspects of convective heat transfer. Springer, New York
22. Jena SK, Mathur MN (1981) Similarity solutions for laminar free convection flow of a thermo-micropolar fluid past a nonisothermal flat plate. Int J Eng Sci 19:1431–1439
23. Guram GS, Smith AC (1980) Stagnation flows of micropolar fluids with strong and weak interactions. Comput Math Appl 6:213–233
24. Ahmadi G (1976) Self-similar solution of incompressible micropolar boundary layer flow over a semi-infinite flat plate. Int J Eng Sci 14:639–646
25. Peddieson J (1972) An application of the micropolar fluid model to the calculation of turbulent shear flow. Int J Eng Sci 10:23–32